Eur. J. Biochem. **269**, 4938–4947 (2002) © FEBS 2002 doi:10.1046/j.1432-1033.2002.03194.x

Probing the role of glutamic acid 139 of *Anabaena* ferredoxin-NADP$^+$ reductase in the interaction with substrates

Merche Faro[1], Susana Frago[1], Tomas Mayoral[2], Juan A. Hermoso[2], Julia Sanz-Aparicio[2], Carlos Gómez-Moreno[1] and Milagros Medina[1]

[1]*Departamento de Bioquímica y Biología Molecular y Celular, Facultad de Ciencias, Universidad de Zaragoza, Spain;* [2]*Grupo de Cristalografía Macromolecular y Biología Estructural, Instituto Química-Física Rocasolano, C.S.I.C. Serrano 119, Madrid, Spain*

The role of the negative charge of the E139 side-chain of *Anabaena* Ferredoxin-NADP$^+$ reductase (FNR) in steering appropriate docking with its substrates ferredoxin, flavodoxin and NADP$^+$/H, that leads to efficient electron transfer (ET) is analysed by characterization of several E139 FNR mutants. Replacement of E139 affects the interaction with the different FNR substrates in very different ways. Thus, while E139 does not appear to be involved in the processes of binding and ET between FNR and NADP$^+$/H, the nature and the conformation of the residue at position 139 of *Anabaena* FNR modulates the precise enzyme interaction with the protein carriers ferredoxin (Fd) and flavodoxin (Fld). Introduction of the shorter aspartic acid side-chain at position 139 produces an enzyme that interacts more weakly with both ET proteins. Moreover, the removal of the charge, as in the E139Q mutant, or the charge-reversal mutation, as in E139K FNR, apparently enhances additional interaction modes of the enzyme with Fd, and reduces the possible orientations with Fld to more productive and stronger ones. Hence, removal of the negative charge at position 139 of *Anabaena* FNR produces a deleterious effect in its ET reactions with Fd whereas it appears to enhance the ET processes with Fld. Significantly, a large structural variation is observed for the E139 side-chain conformer in different FNR structures, including the E139K mutant. In this case, a positive potential region replaces a negative one in the wild-type enzyme. Our observations further confirm the contribution of both attractive and repulsive interactions in achieving the optimal orientation for efficient ET between FNR and its protein carriers.

Keywords: catalytic mechanism; electron transfer; ferredoxin-NADP$^+$ reductase; protein–protein interaction.

During the photosynthetic light-driven reactions solar energy is converted into chemical energy and stored in the cell in the form of ATP and NADPH reducing equivalents. Ferredoxin-NADP$^+$ reductase (FNR, EC 1.18.1.2) is an FAD containing flavoenzyme that catalyses the electron transfer (ET) from each of two molecules of the one electron carrier ferredoxin (Fd), and uses them to convert NADP$^+$ into NADPH via hydride (H^-) transfer from the N5 of the FAD isoalloxazine ring to the NADP$^+$ nicotinamide ring, according to the reaction:

$$2Fd_{rd} + NADP^+ + H^+ \overset{FNR}{\longleftrightarrow} 2Fd_{ox} + NADPH$$

Correspondence to M. Medina, Departamento de Bioquímica y Biología Molecular y Celular, Facultad de Ciencias, Universidad de Zaragoza, 50009-Zaragoza, Spain.
Fax: + 34 976762123, Tel.: + 34 976762476,
E-mail: mmedina@posta.unizar.es

Abbreviations: FNR, ferredoxin-NADP$^+$ reductase; FNR_{ox}, FNR in the oxidized state; FNR_{rd}, FNR in the reduced state; FNR_{sq}, FNR in the semiquinone state; Fd, ferredoxin; Fd_{ox}, Fd in the oxidized state; Fd_{rd}, Fd in the reduced state; Fld, flavodoxin; Fld_{ox}, Fld in the oxidized state; Fld_{rd}, Fld in the reduced state; ET, electron transfer; DCPIP, 2,6-dichloroindophenol.

Enzymes: ferredoxin-NADP$^+$ reductase (FNR; EC 1.18.1.2).

(Received 6 June 2002, revised 13 August 2002, accepted 21 August 2002)

In cyanobacteria and certain algae when the organism is grown under iron deficient conditions flavodoxin (Fld) is synthesized instead of Fd and replaces it in the ET from photosystem I to FNR [1,2]. Three-dimensional structures of free FNRs from different organisms have been reported [3–6], as well of those of nonproductive complexes with NADP$^+$ [3,7]. FNR has also been shown to be a prototype for a large family of flavin-dependent oxidoreductases that function as transducers between nicotinamide dinucleotides (two-electron carriers) and various one-electron carrier proteins [4,5,8]. Moreover, recently, the structures of biologically relevant FNR_{ox} : Fd_{ox} complexes, in *Anabaena* and maize, have been solved [9,10], whereas no structures concerning the FNR interaction with Fld have been reported.

In *Anabaena* FNR it has been shown that electrostatic interactions contribute to the stabilization of a 1 : 1 complex with either Fd or Fld [11–13]. Thus, it is proposed that both ET proteins occupy the same region for the interaction with the reductase, although each individual residue on FNR does not appear to participate to the same extent in the different processes with Fd and Fld [14]. A wide range of results is consistent with a plus–minus electrostatic interaction in which FNR contributes with basic residues, while the ET protein contributes with acidic ones, to the stabilization of the complex [13–18]. Nevertheless, in the FNR : Fd complex it has been proven that these are not the only forces involved in the ET interaction and a crucial role has been established for some hydrophobic residues in optimal binding and orientation for efficient ET [19,20]. The crystal structure of the *Anabaena* FNR : Fd

complex is consistent with both the electrostatic nature of the interaction as well as the critical contribution of hydrophobic interactions to the binding specificity [9]. Moreover, the structure of FNR suggested that not only positive charges, but also some negative ones, might play an important role at the Fd interaction surface. Thus, site-directed mutagenesis studies indicated that the carboxylate group of E301 in FNR plays a critical role in the redox processes between the isoalloxazine moiety of FAD and Fd or Fld [21], probably by stabilizing the flavin semiquinone intermediate while transferring protons from the external medium to the FNR isoalloxazine N5 atom through S80 [3,5,21]. E301A FNR showed important altered properties with regard to wild-type FNR, which were ascribed to structural differences in the microenvironment of the isoalloxazine ring [21,22]. Moreover, the structure of E301A FNR also showed interesting conformational changes in the side-chain of another glutamic acid residue, E139, that in the mutant points towards the FAD cofactor in the active centre cavity and is stabilized by a network of hydrogen bonds that connects it to the flavin ring through the S80 side-chain [22]. Such observation also suggested that in E301A FNR the side-chain of E139 might influence the properties of the flavin, assuming some of the functions carried out by E301 in the wild-type enzyme [22]. In this context, a special reactivity of the side-chain of E139 had already been shown [23]. Therefore, since in *Anabaena* FNR, E301 and E139 are the only negatively charged side-chains exposed around the putative ET protein-binding site, it is worthwhile to analyse the function of the glutamic acid residue at position 139. A previous characterization of the reduction of several E139 FNR mutants by Fd suggested the formation of less productive complexes induced by nonconservative replacements at E139, which were responsible for the impairment in accepting electrons from Fd at low ionic strength (μ) [24]. In the present study, further characterization of E139D, E139K and E139Q FNR forms has been carried out in order to elucidate the role of E139 not only in the protein interaction and ET with Fd, but also with the other two FNR substrates, Fld and $NADP^+$. Kinetic data will be used together with the three-dimensional structure of E139K FNR to reveal the function of this versatile glutamic acid residue in the interaction of FNR with its substrates.

MATERIALS AND METHODS

Biological material

Wild-type, E139K, E139Q and E139D forms from *Anabaena* PCC 7119 FNR were produced as described previously [24]. UV–visible absorption spectroscopy and SDS/PAGE were used as purity criteria.

Steady-state kinetic analysis

The FNR diaphorase, assayed with 2,6-dichloroindophenol (DCPIP) as electron acceptor, and the FNR NADPH-dependent cytochrome *c* reductase, using either Fd or Fld as protein electron carrier, activities were determined for all of the FNR mutants in 50 mM Tris/HCl pH 8.0 at 25 ± 1 °C as described [21,25]. Ionic strength was adjusted by adding aliquots of a 5 M NaCl to each standard reaction mixture.

Stopped-flow kinetic measurements

Fast ET processes between the different FNR forms, either in the oxidized or reduced states, and its substrates (Fd, Fld and NADPH), were studied by stopped-flow methodology under anaerobic conditions using an Applied Photophysics SX17.MV spectrophotometer interfaced with an Acorn 5000 computer using the SX18.MV software from Applied Photophysics [21]. The observed rate constants (k_{obs}) were calculated by fitting the data to a mono- or bi-exponential process. Samples were made anaerobic by successive evacuation and flushing with O_2-free Air, before being introduced into the stopped-flow syringes. Equimolecular concentrations of FNR and each of its substrates were used. Final concentrations were kept in the range 10–15 μM. Since the protocol for anaerobic sample production does not allow an exact control of protein concentration, only a qualitative analysis of the amplitudes ascribed to the different processes was performed. Appropriate wavelengths to follow the reaction were chosen for each process taking into account the extinction coefficient changes of both reactants resulting from the processes of oxidation and reduction. Measurements were carried out in 50 mM Tris/HCl, pH 8.0 at 13 ± 1 °C. Each kinetic trace was the mean of 4–10 independent measurements. Errors in the determination of k_{obs} values were ± 10%.

Crystal growth, data collection and structure refinement

Crystals of E139K FNR were grown by the hanging drop method. The 5-μL droplets consisted of 2 μL 0.75 mM protein in 10 mM Tris/HCl pH 8.0, 1 μL β-octylglucoside at 5% (w/v), 18% polyethylene glycol 6000, 20 mM ammonium sulphate and 0.1 M Mes/NaOH pH 5.5. The droplets were equilibrated against 1 mL reservoir solution at 20 °C. Crystals grew to a maximum size of $0.7 \times 0.4 \times 0.4$ mm in the presence of phase separation caused by the detergent. X-ray data for the E139K FNR were collected at 100 K on a Mar Research (Norderstedt, Germany) IP area detector using a graphite monochromatic CuKα radiation generated by an Enraf-Nonius (Delft, the Netherlands) rotating anode generator up to 2.5 Å resolution. The crystal belongs to the $P6_5$ hexagonal space group with unit cell dimensions $a = b = 87.03$ Å and $c = 96.37$ Å. The Vm is 3.3 $Å^3$/Da with one FNR molecule in the asymmetric unit and 63% solvent content. Data were processed and reduced with MOSFLM and SCALA from the CCP4 package [26]. The E139K structure was solved by molecular replacement using the program AMORE [27] on the basis of the 1.8-Å resolution native FNR model [3], without FAD cofactor, SO_4^{2-} anion and water molecules (Table 1). An unambiguous single solution for the rotation and translation functions was obtained, which was refined by the fast rigid-body refinement program FITTING. The model was subjected to alternate cycles of conjugate gradient refinement with the program X-PLOR [28] and manual model building with the software package O [29]. Finally, 202 water molecules were added. The coordinates and structure factors for the E139K FNR mutant have been deposited in the Protein Data Bank (accession number 1GR1).

Table 1. Data collection and refinement statistics.

Data collection	
Temperature (K)	100
X-ray source	Rotating anode
Space group	$P6_5$
Cell a,*b*,*c* (Å)	87.03; 87.03; 96.37
Resolution Range (Å)	27.3–2.5
N°. of unique refections	13944
Completeness of data (%)	
All data	97.1
Outer shell	99.9
R_{sym} [a] (%)	16.7
Refinement statistics	
Sigma cutoff	0
Resolution Range (Å)	10–2.5
N° of protein atoms	2338
N° of heterogen atoms	58
N° of solvent atoms	203
R_{factor} [b]	18%
Free R_{factor}	25%
RMS deviation	
Bond lengths (Å)	0.008
Bond angles (Å)	0.882
Ramachandran outliers	None

[a] $R_{sym} = \Sigma_{hkl} \Sigma_i | I_i - \langle I \rangle | / \Sigma_{hkl} \Sigma_i \langle I \rangle$ [b] $R_{factor} = \Sigma ||F_o| - |F_c|| / \Sigma |F_o|$

RESULTS

Steady-state kinetic parameters of the different FNR forms

The steady-state kinetic parameters of the different FNR mutants at E139 were determined for two reactions catalysed *in vitro* by FNR by fitting the experimental data to the Michaelis–Menten equation.

Diaphorase activity. The analysis of the kinetic parameters of E139K, E139Q and E139D FNR variants determined when using the DCPIP-diaphorase assay yielded values in the same range as those obtained for the wild-type FNR (Table 2). Thus, at the ionic strength range assayed, all of the mutants had K_m^{NADPH} and k_{cat} values that were within a factor of 2 of those of the wild-type enzyme. Increasing the salt concentration produced larger K_m^{NADPH} values for all the FNR forms (between 3- and 5-fold from $\mu = 28$ mM to $\mu = 200$ mM), as expected due to the electrostatic nature of the interaction between FNR and $NADP^+$ [3,30,31]. When analysing the k_{cat} values, the largest effect was found for E139K FNR at $\mu = 28$ mM (50 mM Tris/HCl pH 8.0) that is 72% that of wild-type FNR. Moreover, while the k_{cat} values for E139Q and E139D FNRs diminish with increasing ionic strength similar to those of the wild-type enzyme, the k_{cat} value for the charge reversal mutant, E139K FNR, is salt concentration independent. Thus, when studying the catalytic efficiency for these mutants in the diaphorase reaction, all of them yield values very close to those of the wild-type enzyme at the different ionic strengths assayed (within a factor of 1.5). Moreover, in all cases an important decrease in the efficiency of the assay was observed upon increasing the ionic strength, which, as indicated above, is due mainly to the increases observed in the K_m^{NADPH} values.

NADPH-dependent cytochrome c reductase activity. The effects observed by replacement of E139 in FNR were larger when analysing cytochrome *c* reductase activity (Table 3), where, apart from the interaction and ET

Table 2. Kinetic parameters for wild-type and mutated FNR variants as obtained in the diaphorase assay at different ionic strengths.

Ionic strength (mM)	Wild-type FNR			E139D FNR			E139Q FNR			E139K FNR		
	k_{cat} (s^{-1})	K_m^{NADPH} (μM)	k_{cat}/K_m ($\mu M^{-1}.s^{-1}$)	k_{cat} (s^{-1})	K_m^{NADPH} (μM)	k_{cat}/K_m ($\mu M^{-1}.s^{-1}$)	k_{cat} (s^{-1})	K_m^{NADPH} (μM)	k_{cat}/K_m ($\mu M^{-1}.s^{-1}$)	k_{cat} (s^{-1})	K_m^{NADPH} (μM)	k_{cat}/K_m ($\mu M^{-1}.s^{-1}$)
28	81 ± 3	6.0 ± 0.6	13.5 ± 0.5	89 ± 3	4.7 ± 0.2	19.1 ± 1.2	88 ± 5	3.4 ± 0.2	26.1 ± 3.0	59 ± 1	5.8 ± 0.3	10.2 ± 0.6
100	66 ± 3	7.6 ± 0.3	8.6 ± 0.1	85 ± 2	13.7 ± 1.2	6.3 ± 0.4	76 ± 8	11.6 ± 0.3	6.6 ± 0.6	60 ± 1	9.7 ± 0.2	6.2 ± 0.5
200	54 ± 3	17.8 ± 0.8	3.0 ± 0.3	58 ± 4	29.7 ± 5.9	2.1 ± 0.5	60 ± 4	23.7 ± 2.2	2.5 ± 0.4	63 ± 1	33.4 ± 0.8	1.9 ± 0.1

Table 3. Kinetic parameters for wild-type and mutated FNR variants as obtained in the NADPH-dependent cytochrome *c* reductase assay at different ionic strengths using either Fd or Fld as electron carrier protein.

Ionic strength (mM)	Wild-type FNR			E139D FNR			E139K FNR			E139Q FNR		
	k_{cat} (s^{-1})	K_m (μM)	k_{cat}/K_m ($\mu M^{-1}.s^{-1}$)	k_{cat} (s^{-1})	K_m (μM)	k_{cat}/K_m ($\mu M^{-1}.s^{-1}$)	k_{cat} (s^{-1})	K_m (μM)	k_{cat}/K_m ($\mu M^{-1}.s^{-1}$)	k_{cat} (s^{-1})	K_m (μM)	k_{cat}/K_m ($\mu M^{-1}.s^{-1}$)
Ferredoxin												
28	225 ± 3	23 ± 1	9.7 ± 0.2	280 ± 18	100 ± 13	2.8 ± 0.7	176 ± 5	4.3 ± 1.5	41 ± 9	117 ± 1	0.27 ± 0.01	433 ± 19
100	209 ± 9	20 ± 3	10.4 ± 2.1	192 ± 6	23 ± 2	8.4 ± 0.8	155 ± 10	2.5 ± 0.4	62 ± 11	58 ± 10	0.5 ± 0.1	116 ± 15
200	135 ± 5	21 ± 2	6.4 ± 0.9	148 ± 6	40 ± 4	3.8 ± 0.6	120 ± 8	3.5 ± 0.2	34 ± 8	70 ± 10	0.9 ± 0.4	78 ± 8
Flavodoxin												
28	24 ± 1	33 ± 5	0.7 ± 0.1	38 ± 10	99 ± 6	0.4 ± 0.2	17 ± 1	10 ± 2	1.7 ± 0.1	25 ± 1	2.4 ± 0.1	10.4 ± 0.6
100	19 ± 1	60 ± 9	0.3 ± 0.5	–	–	–	26 ± 2	28 ± 1	0.9 ± 0.1	25 ± 1	10.9 ± 0.6	2.3 ± 0.2
200	14 ± 1	127 ± 23	0.11 ± 0.04	–	–	–	28 ± 4	49 ± 9	0.6 ± 0.1	20 ± 1	26.6 ± 3.1	0.7 ± 0.1

between FNR and NADPH, complex formation and ET between the FNR and the electron carrier protein is required.

Thus, nonconservative replacement of E139 produced large decreases in the K_m values when using Fd as protein carrier (K_m^{Fd}) from FNR to cytochrome *c*. Thus, under the standard conditions ($\mu = 28$ mM), E139K and E139Q FNR variants show K_m^{Fd} values 85- and 5-fold, respectively, lower than that found for the wild-type enzyme. This effect is observed at all ionic strengths assayed and suggests that the presence of a negatively charged residue at this position is in some way involved in weakening the interaction between FNR and Fd. In line with this, the conservative replacement of E139 by aspartic acid produces an increase in the K_m^{Fd} value (more than 4-fold). Moreover, while E139K and E139Q FNRs had k_{cat} values that were 52% and 78%, respectively, of that observed for wild-type enzyme, when assayed under the same conditions ($\mu = 28$ mM), E139D FNR reaches k_{cat} values slightly higher (124%) than that of wild-type enzyme. The dependence of k_{cat} on increasing ionic strength was the same in all of the FNR forms, showing a decrease in the k_{cat} as the salt concentration was increased.

When the FNR NADPH-dependent cytochrome *c* reductase activity was assayed using Fld as protein carrier, the corresponding kinetic parameters were also altered by E139 replacement. However, the magnitudes of the observed changes were smaller than those observed when using Fd. Thus, at the standard conditions ($\mu = 28$ mM), E139K and E139Q FNRs also show K_m values for Fld (K_m^{Fld}) considerably smaller (13- and 3-fold, respectively), than that for wild-type FNR, whereas their corresponding k_{cat} values are similar to that of wild-type. With regard to the ionic strength dependence, the K_m^{Fld} is more sensitive to salt concentration than K_m^{Fd}, leading to K_m^{Fld} values at $\mu = 200$ mM at least 4-fold larger than those obtained at $\mu = 28$ mM, for all mutated and wild-type FNRs. Again, in contrast with the nonconservative replacements, the substitution of E139 by aspartic acid causes a large increase in the K_m^{Fld} value (3-fold with regard to the wild-type) and results in a k_{cat} value 1.6-fold larger than that obtained for wild-type enzyme. Moreover, linear concentration dependencies were observed for E139D at $\mu = 100$ mM and $\mu = 200$ mM in the Fld concentration range studied (up to 150 μM) making it impossible to calculate the corresponding kinetic parameters.

As a direct consequence of the changes observed for the K_m values, either with Fd or Fld, the corresponding catalytic efficiencies (k_{cat}/K_m) are, when compared with the wild-type values, higher for E139K and E139Q FNRs, and slightly smaller for the E139D mutant.

Fast kinetic stopped-flow analysis of the reaction of the different FNR variants with their substrates

Stopped-flow methodology allows further analysis of the time course of association and ET between FNR, either in the oxidized or reduced states, and its substrates (Fd, Fld and NADPH) [21].

Reactions of FNR with $NADP^+$/NADPH. Reduction of the *Anabaena* FNR variants by NADPH and reoxidation of the reduced enzyme by $NADP^+$ were followed by the FNR flavin spectral changes produced at 458 nm. Wild-type FNR reacted rapidly with NADPH, producing a decrease in absorption that was best fit by two processes that have been attributed to the production of the charge-transfer complex [FNR_{ox} : NADPH] ($k_{obs} > 500 \cdot s^{-1}$) followed by the H^- transfer from NADPH to FAD ($k_{obs} > 140 \cdot s^{-1}$), resulting in the equilibrium mixture of both charge-transfer complexes, [FNR_{ox} : NADPH] and [FNR_{rd} : $NADP^+$] [21,32]. The time courses observed for the reduction of the different FNR E139 mutants by NADPH show kinetic profiles that are similar to that of the wild-type enzyme

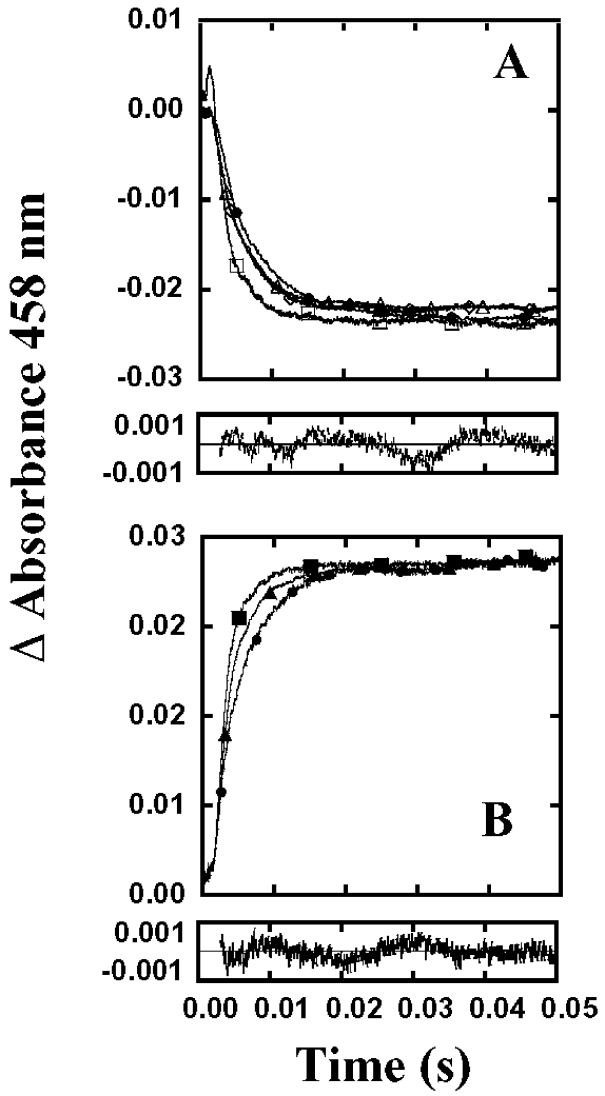

Fig. 1. Time course of the anaerobic reactions of FNR forms with its $NADP^+$/H cofactor as measured by stopped-flow. Reactions were carried out in 50 mM Tris/HCl pH 8.0, at 13 °C and followed at 458 nm. Equimolar concentrations of both reactants were used in the range 10–15 μM. (A) Reaction of FNR_{ox} with NADPH. Also shown is the residual for the fit of the transient corresponding to E139D to a biexponential equation. □, Wild-type FNR; ◇, E139D FNR; △, E139Q FNR; ●, E139K FNR. (B) Reaction of FNR_{rd} with $NADP^+$. Also shown the residual for the fit of the transient corresponding to E139K to a monoexponential process. ■, E139Q FNR; ▲, E139D FNR; ●, E139K FNR.

Table 4. Fast kinetic parameters for the reactions of wild-type and mutated FNR forms with its substrates as studied by stopped-flow methodology. ND, no data available.

	k_{obs} (s^{-1}) for the mixing of FNR_{ox} with			k_{obs} (s^{-1}) for the mixing of FNR_{rd} with		
FNR variant	NADPH[a]	Fd_{rd}[b]	Fld_{rd}[c]	$NADP^+$[a]	Fd_{ox}[b]	Fld_{ox}[c]
Wild-type	> 500[e]	ND[d]	ND[d]	> 550[e]	> 500[e]	2.5
	> 140[e]					0.5
E139D	> 350[e]	ND[d]	ND[d]	250	> 500[a]	4
	> 140[e]					0.7
E139Q	> 350[e]	> 550[e]	ND[d]	348	140	3
	> 140[e]					0.6
E139K	> 330[e]	ND[f]	ND[d]	220	180[e]	17
	> 130[e]	> 370[g] (μ = 133 mM)			13	2.2

[a] Reaction followed at 458 nm. [b] Reaction followed at 507 nm. [c] Reaction followed at 600 nm. [d] Reaction occurred within the dead time of the instrument. [e] Most of the reaction took place within the instrument's dead time. [f] No reaction was detected. [g] Ionic strength was adjusted to 133 mM by adding NaCl from a 5 M stock solution.

(Fig. 1A), and fitting of the kinetic traces shows only slightly slower k_{obs} values for the process ascribed to the formation of the initial charge-transfer complex with regard to that of the wild-type (Table 4). The kinetics of reoxidation of the wild-type enzyme by $NADP^+$ produces an increase in absorbance at 458 nm that is best fit to a single exponential process having a rate constant > 550·s^{-1}. This reaction has been attributed to ET within the complex, i.e. [FNR_{rd} : $NADP^+$] → [FNR_{ox} : NADPH] [21,32]. When analysing this reaction for the different E139 FNR mutants, a fast increase in absorption was also observed, which takes place on the same time scale and with equivalent amplitudes as those observed for the wild-type enzyme reaction (Fig. 1B). Moreover, the observed kinetic traces were all best fit to mono exponential processes with k_{obs} values between 40% (for E139D and E139K) and 64% (for E139Q) of that found for the wild-type enzyme (Table 4). Therefore, although it is not possible to quantify exactly the magnitude of the impairment due to the E139 replacement, considering that equivalent amplitudes are detected for the wild-type and the mutants' processes, it appears that only subtle changes have occurred for the overall interaction process between FNR and its coenzyme in both redox states.

Reactions of FNR with Fd. Reactions between FNR and Fd were followed at 507 nm; this wavelength is an isosbestic point for FNR_{ox} and FNR_{sq} and, although it is not an isosbestic point for FNR_{sq} and FNR_{rd}, the absorbance change associated with the FNR_{sq} → FNR_{rd} transition is negligible when compared with that due to the redox state change of Fd at this wavelength. When following the ET process between Fd_{rd} and FNR_{ox} no reaction was detected in the cases of the wild-type or the E139D FNRs. Previous transient kinetic studies predict k_{obs} values for both wild-type and E139D FNRs to be > 1000·s^{-1} for the ET between FNR_{ox} and Fd_{rd} to produce FNR_{sq} and Fd_{ox} [24], and thus under our stopped-flow experimental conditions the reaction should occur within the instrument's dead time. Moreover, previous stopped-flow experiments performed with wild-type FNR and a 3-fold excess of Fd_{rd} [21] showed evidence of a fast reaction (k_{obs} > 250·s^{-1}) which was ascribed to the reoxidation of a second molecule of Fd_{rd} by the FNR_{sq}, expected to have been rapidly formed within the stopped-flow experimental dead time. However, because under our present experimental conditions FNR and Fd are mixed in equimolecular amounts, there is no Fd_{rd} in excess and this second-sequential reaction is not likely to occur. Moreover, according to the thermodynamic driving force of the reaction, the reoxidation of Fd_{rd} ($E = -384$ mV) by FNR ($E = -323$ mV) [33] is expected to take place completely and no Fd_{rd} would be in equilibrium with the rapidly formed products Fd_{ox} and FNR_{sq}. For the reaction between Fd_{rd} and E139Q FNR, we were able to observe only the final traces of the Fd reoxidation to which corresponds a k_{obs} > 550·s^{-1} indicating that this process has been affected to some degree although we are not able to quantify it. No reaction was detected also for the ET from Fd to E139K FNR. However, taking into account the large impairment reported for the E139K mutant in accepting electrons from Fd at low ionic strength [24], the lack of observable reaction in this particular case must be attributed to the fact that the reaction does not take place at all under our stopped-flow conditions. In order to confirm this hypothesis, and to rule out the possibility of the reaction taking place within the instrument's dead time, it was followed at higher salt concentration. A process observed at μ = 133 mM and having a k_{obs} > 370·s^{-1} (Fig. 2A) was ascribed to the reduction of the mutant by Fd_{rd}. This final ionic strength was chosen so that the expected process could be detected after taking into account the k_{obs} values reported previously for the ET from Fd_{rd} and E139K FNR_{ox} when the reaction was measured by laser flash photolysis (Fig. 3 [24]).

When the reverse reaction, i.e. ET from FNR_{rd} to Fd_{ox} was studied, different behaviours were also observed for the E139 FNR mutants (Fig. 2B). Reduction of Fd by wild-type FNR, although mostly limited by the instrument's dead time, yielded a decay at 507 nm which corresponded to a k_{obs} > 500·s^{-1}. E139D FNR reacts in a manner indistinguishable from wild-type, whereas E139Q FNR shows a k_{obs} of 140·s^{-1}, demonstrating that neutralization of the negative charge at position 139 produces a sizeable impairment on the enzyme ET to Fd. Again, E139K FNR was, by far, the most impaired in its ET to

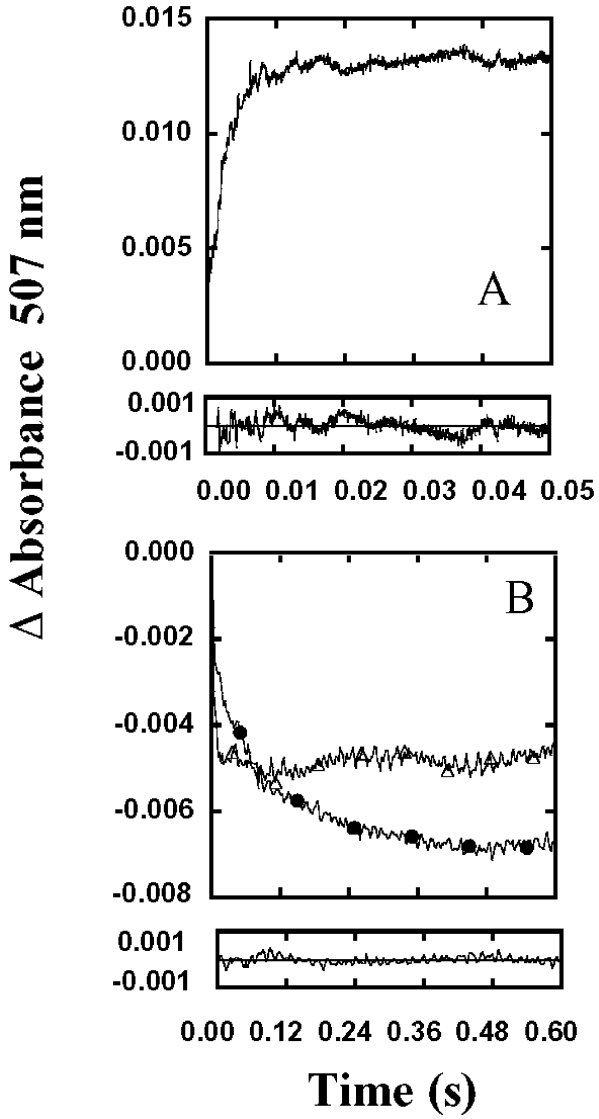

Fig. 2. Time course of the anaerobic reactions of FNR forms with Fd as measured by stopped-flow. Reactions were carried out in 50 mM Tris/HCl pH 8.0, at 13 °C and followed at 507 nm. Equimolar concentrations of both reactants were used in the range 10–15 μM. (A) Reaction of E139K FNR_{ox} with Fd_{rd}. In this particular case ionic strength has been adjusted to 133 mM by adding NaCl; also shown is the residual for the fit to a monoexponential process. (B) Reaction of FNR_{rd} with Fd_{ox}. △, E139Q; ●, E139K FNR; also shown is the residual for the fit of the E139K transient to a biexponential process.

Fd, yielding kinetic transients which, strikingly, were best fit to a biexponential process showing a fast phase with a k_{obs} of $180 \cdot s^{-1}$ and a much slower phase with a k_{obs} of $13 \cdot s^{-1}$ (Fig. 2B).

Reactions of FNR with Fld. These processes were followed mainly at 600 nm to observe production of both Fld and FNR semiquinone forms. As previously reported, the time course of wild-type FNR reduction by Fld_{rd} cannot be followed under these conditions due to the fact that it occurs within the instrument's dead time [21]. None of the E139 FNR mutants show any detectable absorbance change in this reaction, which suggests again that the reactions were too fast to be followed under our stopped-flow conditions.

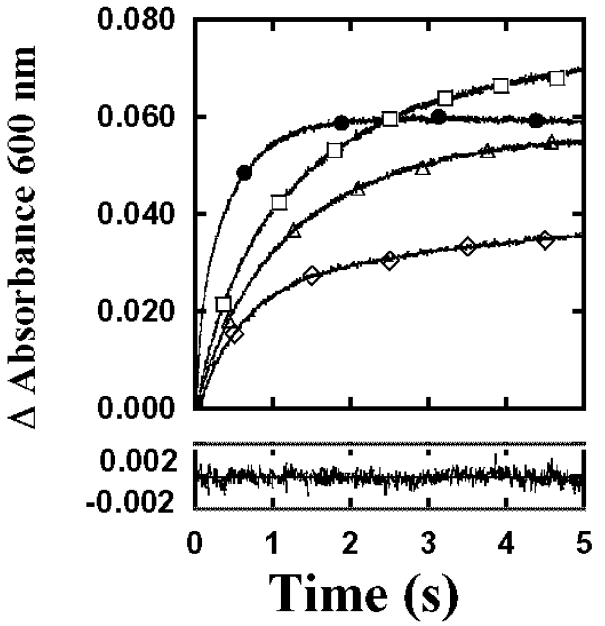

Fig. 3. Time course of the anaerobic reactions of reduced FNR forms with Fld_{ox} as measured by stopped-flow. Reactions were carried out in 50 mM Tris/HCl pH 8.0, at 13 °C. Equimolar concentrations of both reactants were used in the range of 10–15 μM; □, wild-type FNR; ◇, E139D FNR; △, E139Q FNR; ●, E139K FNR. Also shown is the residual for the biexponential fit of the transient corresponding to the wild-type reaction.

As observed for the reaction between wild-type FNR_{rd} and Fld_{ox}, two phases were also detected for all the mutants (Fig. 3). E139D FNR and E139Q FNR show wild-type like behaviour and only subtle changes in the corresponding rate constants were observed (Table 4). Although no major changes were observed for this process upon replacement of E139 by lysine, it is noticeable that E139K FNR resulted in the maximal efficiency for this process exhibiting significant increments on the respective observed rate constants ($17 \cdot s^{-1}$ vs. $2.5 \cdot s^{-1}$ for k_{obs1} and $2.2 \cdot s^{-1}$ vs. $0.5 \cdot s^{-1}$ for k_{obs2}). Fitting the 600 nm traces for all the FNR forms yield equivalent amplitudes, with the amplitude for the slower process being 2- to 4-fold larger than that of the faster process for all of the mutants.

Three-dimensional structure of the E139K FNR mutant

The three-dimensional structure of the E139K FNR mutant has been determined by X-ray diffraction. The first eight residues in the sequence were not included in the model due to the poor electron density map in this region. The overall folding of the mutant shows no significant differences with respect to the native structure, as shown by the very low rmsd (0.22 Å) of the Cα backbone. Only slight differences are observed in the loop starting at Y104 and ending at V113 near the region interacting with the adenine moiety of FAD, but they are not significant due to the poor definition of the electron density map in this region for all FNR forms

[3,9,18,22]. No structural changes in the Cα backbone at the mutated position were observed. This is surely a consequence of the fact that the 139 position is just at the end of the FAD binding domain (residues 1–137), a region very well stabilized by a scaffold of six antiparallel strands arranged in two perpendicular β-sheets. The K139 residue is well defined in the electron density map, although some chain mobility is detected as shown by a higher thermal atomic factor for side-chain atoms (averaged *B*-value of 32 $Å^2$) as compared with the other side-chains in the region. K139 exhibits a change in the side-chain conformation compared to the E139 conformer observed in the wild-type enzyme (Fig. 4A). A large structural variation has also been observed for the E139 conformer in the different *Anabaena* FNR structures reported previously (Fig. 4). Finally, a strong polarity change in the FAD environment is introduced by the E139K mutation, creating an area with positive potential in a region with a marked acidic character in the wild-type enzyme (data not shown, see Fig. 1 in [24]).

DISCUSSION

Analysis of the FNR diaphorase kinetic parameters indicates that replacement of E139 by aspartic acid, glutamine or lysine, alters k_{cat} and K_m^{NADPH} only slightly. Moreover, the increases in the K_m^{NADPH} value for all of the mutants with ionic strength are consistent with long-range electrostatic interactions being weakened [30,31]. Only in the case of E139K FNR is the k_{cat} value salt independent and slightly decreased with regard to that of the wild-type, although still being significantly reduced by NADPH (Table 2). However, the observed differences induced by the salt may only be the result of a small conformational change occurring in the productive intermediate [FNR_{ox} : NADPH] complex when produced with the mutated enzyme. These results are consistent with those obtained upon analysing the k_{obs} for the fast kinetic reduction of FNR by NADPH, which indicate that all of the E139 FNR mutants accept electrons from NADPH with rates similar to that of the WT (Table 4). The k_{obs} values obtained for the reversal process, [FNR_{rd} : $NADP^+$] → [FNR_{ox} : NADPH], with the different FNR mutants are only slightly lower than the wild-type (Table 4). Therefore, our data indicate that replacement of E139 FNR by glutamic acid, glutamine or lysine produces only subtle changes in the interaction and ET processes between FNR and its coenzyme in both redox states.

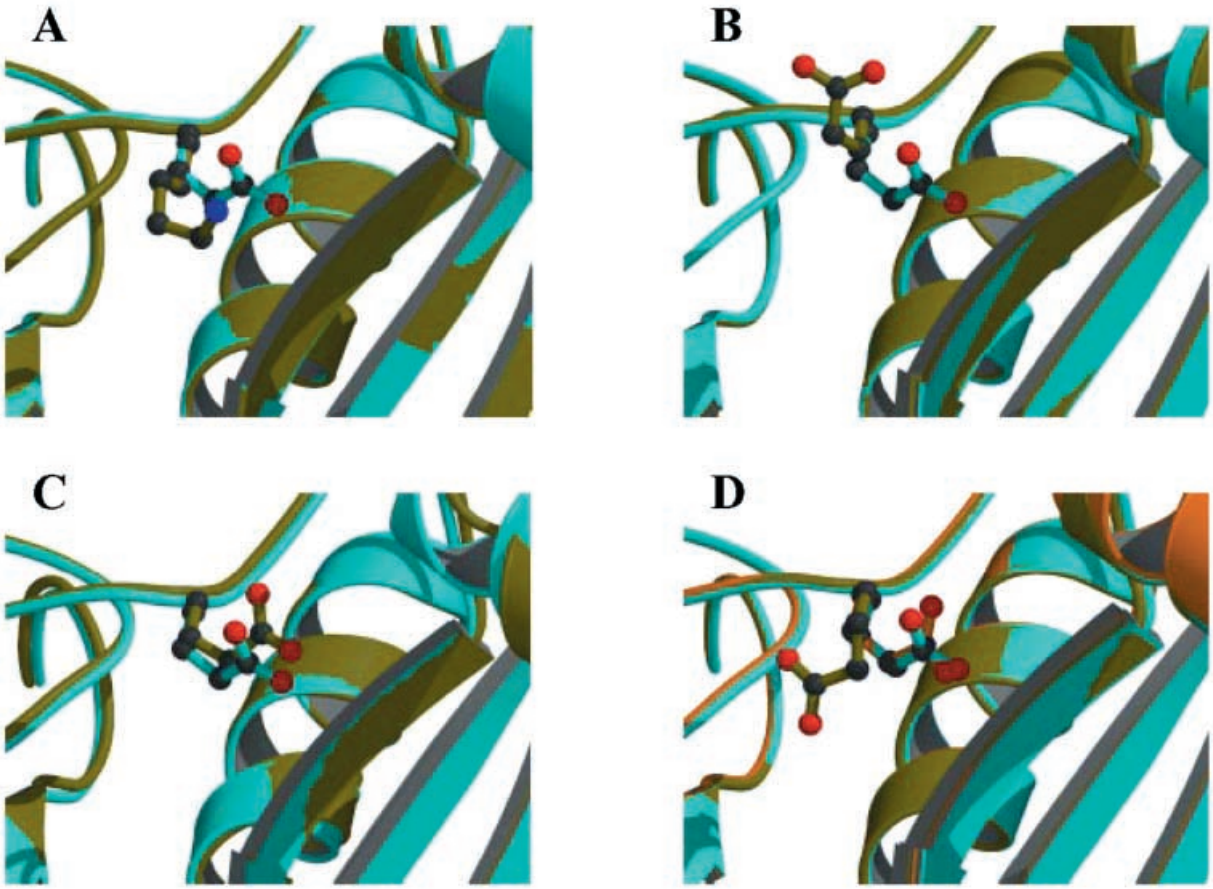

Fig. 4. Three-dimensional structure comparison of the Glu139 conformer in *Anabaena* FNR models. (A) Superposition of wild-type FNR (cyan) with E139K FNR mutant (green). (B) E139 presents a very different conformation in the FNR:$NADP^+$ complex (green) as compared with the wild-type FNR (cyan). (C) A more similar conformation for E139 is observed for the wild-type FNR (cyan) and for the FNR:Fd complex (green). (D) E139 conformers as observed in the E301A FNR mutant (green), R264E FNR mutant (orange) and wild-type FNR (cyan). This figure was drawn using MOLSCRIPT [39] and RENDER [40].

The effects observed in the wild-type FNR K_m values for both protein carriers, Fd and Fld, upon increasing ionic strength (Table 3) indicates that the salt debilitates the productive FNR_{rd} : Fld_{ox} interaction but not the FNR_{rd} : Fd_{ox} one. Moreover, lower k_{cat} values for both Fd and Fld are observed upon increasing the ionic strength. This can be ascribed to a shielding of the FNR : coenzyme and FNR : protein carrier electrostatic interactions by salt ions [14]. When studying the corresponding kinetic parameters for the E139 FNR mutants, different effects are observed depending on the nature of the replacement (Table 3). As only negligible effects upon E139 replacement have been observed in the FNR kinetic parameters for the diaphorase assay (Table 2), such differences must be due to the effect introduced by the mutation in the FNR : protein carrier interaction. Thus, conservative replacement of E139 by aspartic acid, apparently produced an enzyme which exhibited considerably larger K_m^{Fd} and K_m^{Fld} values, while having k_{cat} values slightly larger than those of the wild-type enzyme, which in the case of Fd decrease with increasing ionic strength, like the wild-type process. Moreover, when analysing by fast kinetic methods the ability of E139D FNR to accept or to transfer electrons with either Fd or Fld, the time scale of the overall process is not affected by the mutation (Table 4). Such observations suggest that the side-chain of residue 139 must be involved in the precise orientation of the complex, and that the shorter aspartic acid side-chain provides an electrostatic interaction with either Fd or Fld that, although weaker, favours the ET process itself.

Charge reversal replacement of E139 FNR produced noticeable effects in the reactions with either Fd or Fld. Considerably lower K_m^{Fld} and, especially, K_m^{Fd} values relative to wild-type FNR were obtained (Table 3). However, the k_{cat} values, which account for the reactivity within the enzyme–intermediate complexes, are considerably smaller with Fd but relatively similar with Fld, when compared to the wild-type. This observation is also consistent with the much lower k_{obs} values obtained by fast kinetic methods for reaction of E139K FNR_{rd} with Fd_{ox}, and the similar values for the reaction of wild-type FNR_{rd} with Fld_{ox} (Table 4). Hence, when Fd is used as protein carrier, the decrease of the E139K FNR K_m values are not accompanied by faster ET. Thus, although the efficiency of the reaction (k_{cat}/K_m) results considerably increased the turnover of the process has decreased by the introduced mutation. This might be due either to a much higher affinity to Fd of the E139K FNR or to the formation of a less productive complex. No major changes have been reported in the K_d values for the [E139K FNR_{ox} : Fd_{rd}] and [E139K FNR_{ox} : Fd_{ox}] complexes with regard to the corresponding ones with wild-type FNR [24], suggesting that probably no changes should be expected in the K_d value for the FNR_{rd} : Fd_{ox} interaction. On the other hand, we have recently reported on less reactive modes of binding at low ionic strength induced by the E139 → K139 substitution [24]. Therefore, formation of additional intermediate complexes must be considered. The fact that the k_{cat}/K_m^{Fd} values for E139K FNR increase considerably with regard to those of the wild-type indicates that in at least one of those intermediate complexes ET can be achieved [34]. A minimal mechanism with at least two productive intermediate complexes might be proposed for the E139K FNR : Fd interaction:

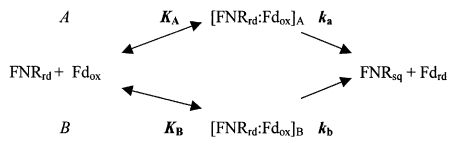

where the reaction rate would depend upon the formation of both intermediate complexes (the dissociation constant ratio, K_A/K_B) and on the two ET rate constants (k_a and k_b). Thus, the effect of such a second productive binding mode would be to make the K_m lower (because a tighter productive binding mode comes into play), to decrease the k_{cat} (because at saturation the second complex must yield a slower turnover number), and to increase the catalytic efficiency (as the two former effects are not altered in a compensatory manner). Such an additional interaction between FNR_{rd} and Fd_{ox} would be also suggested by fast kinetic analysis of the reaction between E139K FNR_{rd} and Fd_{ox} (Table 4), which results not only in severely hindered ET but also in a process best fit to a biexponential, unlike the monoexponential process observed with all other FNR forms assayed thus far [13,14,18,20,21]. Therefore, the two k_{obs} values might correspond to the simultaneous processes of E139K FNR reoxidation by Fd through both complexes. The analysis of the E139K FNR kinetic cytochrome *c* assay parameters with Fd suggests that although the second complex is produced at all ionic strengths assayed, it is greatly weakened by the salt, suggesting that electrostatic interactions are specifically debilitated in this low-reactivity mode of binding. Finally, when analysing the fast reduction of E139K FNR by Fd_{rd}, while no reaction was observed at all at low ionic strength (Table 4), increasing the ionic strength up to 133 mM clearly resulted in efficient reduction of E139K, again suggesting the formation of nonproductive complexes at low ionic strengths. This explanation would be consistent with previous studies of E139K reduction by Fd_{rd} under pseudo-first order conditions ($[Fd_{rd}] \ll [FNR_{ox}]$), which indicated a collisional ternary interaction between FNR_{ox} and a nonoptimal preformed [Fd_{rd} : FNR_{ox}] complex [24]. Alternative binding modes between protein pairs, resulting in different reactivities have also been reported in other systems [35]. Therefore, it is not unexpected that the surface potential change of one of the partners might also produce a different coupling of the redox cofactors involved in the interaction, which might cause a different efficiency in ET.

When the E139K FNR reactivity was assayed using Fld as protein carrier, a salt-dependent decrease in the K_m^{Fld} values was also observed relative to that of the wild-type FNR, although in this case the decrease is one order of magnitude smaller than when using Fd (Table 3). The k_{cat} values are not altered relative to those of the wild-type, even at high salt concentrations. Analysis of fast kinetic reactions shows that E139K FNR is able to transfer electrons to Fld faster than the wild-type enzyme, while behaves similarly in the reverse process (Table 4). Therefore, when using Fld no additional complexes seem to be induced by replacement of E139 FNR by lysine, but rather the mutation might be producing a stronger optimal interaction with the protein that favours the ET process itself.

The kinetic data obtained for all of the processes analysed with E139Q FNR have values intermediate of those described for the E139K mutant and the wild-type FNRs. Thus, the k_{cat} and K_m^{Fd} steady-state parameters and the k_{obs} for the fast ET processes with Fd suggest that in the case of the E139Q mutant formation of the alternative complex might be also achieved. However, its K_B would be larger than that for the complex with E139K FNR and produce a smaller shift of all the steady-state kinetic parameters. Such intermediate behaviour is also observed in the reactions of E139Q FNR with Fld. These results suggest that neutralization of the charge at position 139 also neutralizes any repulsive or attractive interactions involving either glutamic acid or lysine. Therefore, it must be the charge located at 139 and not the H-bond capability that is critical at this residue position.

In the three-dimensional structure reported for the *Anabaena* FNR:Fd complex the E139 FNR side-chain is not making any direct contact with Fd, but is not situated far away from the interaction surface [9]. Moreover, different conformers for the E139 side-chain have been found, not only in the E301A mutant but also in the structures of the R264E mutant and those of the WT FNR complexes with either Fd or $NADP^+$ (Fig. 4) [3,9,18,22]. Thus, this conformational flexibility of E139 side-chain would allow its implication in the reorganization process that takes place upon the initial approach of the proteins, and therefore, may explain why different side-chains at position 139 might allow different modes of interaction with Fd, which result in different ET reactivities. The requirement of conformational flexibility for optimal ET has been demonstrated by covalent cross-linking of either Fd or Fld to FNR, which lowered the ET rate between these proteins [36–38]. Positive charges around the FAD group of FNR have been shown to contribute to the orientation of the intermediate [FNR:Fd] complex [14,18], and among this is the neighbouring K138 side-chain. The change in the electrostatic potential induced by replacement of E139 induces a stronger positive potential in the region where it is located, which is the only negative potential region around the FAD in the WT. Thus, E139 appears to produce a repulsion of the very negatively charged smaller Fd molecule upon initial collision, focusing Fd toward the positive region of FNR, which is closer to the flavin ring of the FAD group, thereby favouring formation of an optimal complex for ET. We conclude that E139 seems to be involved in optimizing the mutual orientation of the redox cofactors by means of electrostatic repulsion, which in turn determines ET rates. Thus far, no structure for a complex between FNR and Fld has been reported. Nevertheless, it is assumed that FNR uses the same site for the interaction with Fd and Fld, although each individual residue does not appear to participate to the same extent in the processes with both protein carriers [14]. Moreover, our data clearly suggest that in the FNR:Fd interaction, replacement of residue 139 produces very different effects compared to those produced in the FNR:Fld one. Thus, the larger local positive potential in the 138–139 region of FNR induced upon elimination of the negative charge at position 139 seems to have a marked stabilizing effect for a productive FNR:Fld interaction. In summary, our results indicate that E139 is not involved in the processes of binding and ET between FNR and $NADP^+$/H, while the nature of the charge and the conformation of the side-chain at position 139 of *Anabaena* FNR modulates the precise enzyme interaction with the protein carriers.

ACKNOWLEDGEMENTS

We are grateful to J.K. Hurley and G. Tollin (University of Arizona) for their collaboration in dicussing different aspects of this work. This work was supported by grant BIO2000-1259 from Comisión Interministerial de Ciencia y Tecnología to C.G.-M and by grant P006/2000 from Diputación General de Aragón to M.M.

REFERENCES

1. Mayhew, S.G. & Tollin, G. (1992) General properties of flavodoxins. In *Chemistry and Biochemistry of Flavoenzymes*, Vol. III (Müller, F., ed.), pp. 389–426. CRC Press, Boca Raton.
2. Rogers, L.J. (1987) Ferredoxins, flavodoxins and related proteins. structure, function and evolution. In *The Cyanobacteria*. (Fay, P. & Van Baalen, C., eds), pp. 35–67. Elsevier Science Publishers, Amsterdam, the Netherlands.
3. Serre, L., Vellieux, F.M.D., Medina, M., Gómez-Moreno, C., Fontecilla-Camps, J.C. & Frey, M. (1996) X-ray structure of the ferredoxin: $NADP^+$ reductase from the cyanobacterium *Anabaena* PCC 7119 at 1.8 Å resolution, and crystallographic studies of $NADP^+$ binding at 2.25 Å resolution. *J. Mol. Biol.* **263**, 20–39.
4. Karplus, P.A., Daniels, M.J. & Herriot, J.R. (1991) Atomic structure of ferredoxin-$NADP^+$ reductase: Prototype for a structurally novel flavoenzyme family. *Science* **251**, 60–66.
5. Bruns, C.M. & Karplus, P.A. (1995) Refined crystal structure of spinach ferredoxin reductase at 1.7 Å resolution: oxidized, reduced and 2′-phospho-5′-AMP bound states. *J. Mol. Biol.* **247**, 125–145.
6. Dorowski, A., Hofmann, A., Steegborn, C., Boicu, M. & Huber, R. (2001) Crystal structure of paprika ferredoxin-$NADP^+$ reductase. Implications for the electron transfer pathway. *J. Biol. Chem.* **276**, 9253–9263.
7. Deng, Z., Aliverti, A., Zanetti, G., Arakaki, A.K., Ottado, J., Orellano, E.G., Calcaterra, N.B., Ceccarelli, E.A., Carrillo, N. & Karplus, A. (1999) A productive $NADP^+$ binding mode of ferredoxin-$NADP^+$ reductase revealed by protein engineering and crystallographic studies. *Nature Struct. Biol.* **6**, 847–853.
8. Correll, C.C., Ludwig, M.L., Bruns, C.M. & Karplus, P.A. (1993) Structural prototypes for an extended family of flavoprotein reductases: Comparison of phthalate dioxygenase reductase with ferredoxin reductase and ferredoxin. *Protein Sci.* **2**, 2112–2133.
9. Morales, R., Charon, M.-H., Kachalova, G., Serre, L., Medina, M., Gómez-Moreno, C. & Frey, M. (2000) A redox-dependent interaction between two electron-transfer partners involved in photosynthesis. *EMBO Reports* **1**, 271–276.
10. Kurisu, G., Kusunoki, M., Katoh, E., Yamazaki, T., Teshima, K., Onda, Y., Kimata-Ariga, Y. & Hase, T. (2001) Structure of the electron transfer complex between ferredoxin and ferredoxin-$NADP^+$ reductase. *Nature Struct. Biol.* **8**, 117–121.
11. Sancho, J. & Gómez-Moreno, C. (1991) Interaction of ferredoxin-$NADP^+$ reductase from *Anabaena* with its substrates. *Arch. Biochem. Biophys.* **210**, 231–233.
12. Fillat, M.F., Edmonson, D.E., & Gómez-Moreno, C. (1990) Structural and chemical properties of a flavodoxin from *Anabaena* PCC7119. *Biochem. Biophys. Acta.* **104**, 301–307.
13. Martínez-Júlvez, M., Medina, M., Hurley, J.K., Hafezi, R., Brodie, T., Tollin, G. & Gómez-Moreno, C. (1998) Lys75 of *Anabaena* ferredoxin-$NADP^+$ reductase is a critical residue for binding ferredoxin and flavodoxin during electron transfer. *Biochemistry* **37**, 13604–13613.
14. Martínez-Júlvez, M., Medina, M. & Gómez-Moreno, C. (1999) Ferredoxin-$NADP^+$ reductase uses the same site for the

interaction with ferredoxin and flavodoxin. *J. Biol. Inorg. Chem.* **4**, 568–578.
15. Hurley, J.K., Salamon, Z., Meyer, T.E., Fitch, J.C., Cusanovich, M.A., Markley, J.L., Cheng, H., Xia, B., Chae, Y.K., Medina, M., Gómez-Moreno, C. & Tollin, G. (1993) Amino acid residues in *Anabaena* ferredoxin crutial to interaction with ferredoxin-$NADP^+$ reductase: site-directed mutagenesis and laser flash photolysis. *Biochemistry* **32**, 9346–9354.
16. Hurley, J.K., Medina, M., Gómez-Moreno, C. & Tollin, G. (1994) Further characterization by site-directed mutagenesis of the protein–protein interface in the ferredoxin/ferredoxin: $NADP^+$ reductase system from *Anabaena*: requirement of a negative charge at position 94 in ferredoxin for rapid electron transfer. *Arch. Biochem. Biophys.* **312**, 480–486.
17. Hurley, J.K., Schmeits, J.L., Genzor, C., Gómez-Moreno, C. & Tollin, G. (1996) Charge reversal mutations in a conserved acidic patch in *Anabaena* ferredoxin can attenuate or enhance electron transfer to ferredoxin: $NADP^+$ reductase by altering protein/protein orientation within the intermediate complex. *Arch. Biochem. Biophys.* **333**, 243–250.
18. Martínez-Júlvez, M., Hermoso, J., Hurley, J.K., Mayoral, T., Sanz-Aparicio, J., Tollin, G., Gómez-Moreno, C. & Medina, M. (1998) Role of Arg100 and Arg264 from *Anabaena* PCC7119 ferredoxin-$NADP^+$ reductase for optimal binding and electron transfer. *Biochemistry* **37**, 17680–17691.
19. Hurley, J.K., Cheng, H., Xia, B., Markley, J.L., Medina, M., Gómez-Moreno, C. & Tollin, G. (1993) An aromatic amino acid is required at position 65 in *Anabaena* ferredoxin for rapid electron transfer to ferredoxin-$NADP^+$ reductase. *J. Am. Chem. Soc.* **115**, 11698–11701.
20. Martínez-Júlvez, M., Nogués, I., Faro, M., Hurley, J.K., Brodie, T.B., Mayoral, T., Sanz-Aparicio, J., Hermoso, J.A., Stankovich, M.T., Medina, M., Tollin, G. & Gómez-Moreno, C. (2001) Role of a cluster of hydrophobic residues near the FAD cofactor in *Anabaena* PCC7119 ferredoxin-$NADP^+$ reductase for optimal complex formation and electron transfer to ferredoxin. *J. Biol. Chem.* **276**, 27498–27510.
21. Medina, M., Martínez-Júlvez, M., Hurley, J.K., Tollin, G. & Gómez-Moreno, C. (1998) Involvement of glutamic acid 301 in the catalytic mechanism of ferredoxin-$NADP^+$ reductase from *Anabaena* PCC7119. *Biochemistry* **37**, 2715–2728.
22. Mayoral, T., Medina, M., Sanz-Aparicio, J., Gómez-Moreno, C. & Hermoso, J.A. (2000) Structural basis of the catalytic role of Glu301 in *Anabaena* PCC 7119 ferredoxin-$NADP^+$ reductase revealed by X-ray crystallography. *Proteins* **38**, 60–69.
23. Bes, M.T., De Lacey, A.L., Peleato, M.L., Fernández, V.M. & Gómez-Moreno, C. (1995) The covalent linkage of a viologen to a flavoprotein reductase transforms it into an oxidase. *Eur. J. Biochem.* **233**, 593–599.
24. Hurley, J.K., Faro, M., Brodie, T.B., Hazzard, J.T., Medina, M., Gomez-Moreno, C. & Tollin, G. (2000) Highly non-productive complexes with *Anabaena* ferredoxin at low ionic strength are induced by nonconservative amino acid substitution at Glu139 in *Anabaena* ferredoxin-$NADP^+$ reductase. *Biochemistry* **39**, 13695–13702.
25. Shin, M. (1971) Ferredoxin-$NADP^+$ reductase from spinach. In *Methods in Enzymology*, Vol. 23 (San Pietro, A., ed.), pp. 440–442. Academic Press, New York, USA.
26. Collaborative Computational Project Number 4. (1994) The CCP.4 suite: programs for protein crystallography. *Acta Crystallogr.* **D50**, 760–763.
27. Navaza, J. (1994) AMoRe: an automated package for molecular replacement. *Acta Crystallogr.* **A50**, 157–163.
28. Brünger, A.T. (1993) *X-PLOR: a System for X-Ray Crystallography and NMR*. Yale University Press, New Haven, CT, USA.
29. Jones, T.A., Zou, J.Y., Cowan, S.W. & Kjeldgaard, M. (1991) Improved methods for building protein models in electron density maps and the location of errors in these models. *Acta Crystallogr.* **A47**, 110–119.
30. Keirns, J.J. & Wang, J.H. (1972) Studies on nicotinamide adenine dinucleotide phosphate reductase of spinach chloroplasts. *J. Biol. Chem.* **247**, 7374–7382.
31. Medina, M., Luquita, A., Tejero, J., Hermoso, J., Mayoral, M., Sanz-Aparicio, J., Grever, K. & Gómez-Moreno, C. (2001) Probing the determinants of coenzyme specificity in ferredoxin-$NADP^+$ reductase by site-directed mutagenesis. *J. Biol. Chem.* **276**, 11902–11912.
32. Batie, C.J. & Kamin, H. (1984) Ferredoxin $NADP^+$ oxidoreductase. Equilibria in binary and ternary complexes with $NADP^+$ and ferredoxin. *J. Biol. Chem.* **259**, 8832–8839.
33. Hurley, J.K., Weber-Main, A.M., Stankovich, M.T., Benning, M.M., Thoden, J.B., Vanhooke, J.L., Holden, H.M., Chae, Y.K., Xia, B., Cheng, H., Markley, J.L., Martínez-Júlvez, M., Gómez-Moreno, C., Schmeits, J.L. & Tollin, G. (1997) Structure–function relationships in *Anabaena* ferredoxin: correlations between X-ray crystal structures, reduction potentials, and rate constants of electron transfer to ferredoxin-$NADP^+$ reductase for site-specific ferredoxin mutants. *Biochemistry* **36**, 11100–11117.
34. Fersht, A. (1999) *Structure and mechanism in protein science*. W.H. Freeman Co., New York, USA.
35. Zhou, J.S., Nocek, J.M., DeVan, M.L. & Hoffman, B.M. (1995) Inhibitor-enhanced electron transfer: copper cytochrome *c* as a redox-inert probe of ternary complexes. *Science* **269**, 204–207.
36. Pueyo, J.J. & Gómez-Moreno, C. (1991) Characterization of the cross-linked complex formed between Ferredoxin-$NADP^+$ reductase and flavodoxin from *Anabaena* PCC7119. *Biochim. Biophys. Acta* **1059**, 149–156.
37. Walker, M.C., Pueyo, J.J., Gómez-Moreno, C. & Tollin, G. (1991) Comparison of the kinetics of reduction and intramolecular electron transfer in electrostactic and covalent complexes of ferredoxin-$NADP^+$ reductase and flavodoxin from *Anabaena* PCC7119. *Arch. Biochim. Biophys.* **281**, 76–83.
38. Zanetti, G., Aliverti, A. & Curti, B. (1984) A cross-linked complex between ferredoxin and ferredoxin-$NADP^+$ reductase. *J. Biol. Chem.* **259**, 6153–6157.
39. Kraulis, P.J. (1991) MOLSCRIPT: a program to produce both detailed and schematic plots of protein structures. *J. Appl. Cryst.* **24**, 946–950.
40. Merritt, E.A. & Bacon, D.J. (1997) Raster3D: Photorealistic Molecular Graphics. *Methods Enzymol.* **277**, 505–524.